

NUMERICAL ANALYSIS ON THE ELECTRIC FIELD IN A
GRADED INDEX FIBER WAVEGUIDE

A THESIS SUBMITTED TO
THE GRADUATE SCHOOL OF NATUREL AND APPLIED SCIENCES
OF
THE MIDDLE EAST TECHNICAL UNIVERSITY

BY
ŞERİFE YAPRAK BALIBEY

IN PARTIAL FULFILLMENT OF THE REQUIREMENTS FOR THE DEGREE
OF MASTER OF SCIENCE
IN
THE DEPARTMENT OF PHYSICS

DECEMBER 2003

Approval of the Graduate School of Natural and Applied Sciences.

Prof. Dr. Canan Özgen
Director

I certify that this thesis satisfies all the requirements as a thesis for the degree of Master of Science.

Prof. Dr. Sinan Bilikmen
Head of Department

This is a certify that we have read this thesis and that in our opinion it is fully adequate, in scope and quality, as a thesis for the degree of Master of Science.

Assoc.Prof.Dr.Serhat Çakır
Supervisor

Examining Committee Members

Prof. Dr. Sinan Bilikmen

Assoc. Prof. Dr. Gülay Öke

Assoc. Prof. Dr. Akif Esendemir

Dr.Ali Alaçakır

Assoc. Prof. Dr. Serhat Çakır

ABSTRACT

NUMERICAL ANALYSIS ON THE ELECTRIC FIELD IN A GRADED INDEX FIBER WAVEGUIDE

Yaprak Balıbey, Şerife

M.Sc., Department of Physics

Supervisor: Assoc. Prof. Dr. Serhat Çakır

December 2003, 52 pages

Propagation of radiation in a waveguides is theoretically described by Maxwell's equations. The gradient of refractive index and an influence on the waveguide by a superstrate requires a numerical solution of the differential equation. Iterative methods such as the Runge-Kutta approaches are used to calculate the effective refractive index in the waveguide depending on the superstrate's and the waveguide's local refractive indices.

In this study, the refractive indices, and the modal fields of the TE_{00} modes are calculated. The calculated fields of the TE_{00} modes give information about the propagation of the light in the waveguide. Also, the precision of the Runge-Kutta approaches has been tested. The advantages and disadvantages of the Runge-Kutta approaches are discussed.

Key Words: Electric field, Waveguide, Numerical Simulation, Runge-Kutta

ÖZ

DERECELİ FİBER DALGA KLAVUZLARINDA ELEKTİRİK ALANININ NÜMERİK ANALİZİ

Yaprak Balıbey, Şerife

Yüksek Lisans, Fizik Bölümü

Tez Yöneticisi: Doç. Dr. Serhat Çakır

Aralık 2003, 52 Sayfa

Dalga klavuzlarının içindeki radyoaktif ışının dağılımı teorik olarak Maxwell denklemleri ile tanımlanır. Kırılma indeksinin değişim ölçüsü ve üst tabakanın dalga klavuzuna etkisi diferansiyel denklemin nümerik çözümünü gerektirir. Tekrarlayıcı metodlar örneğin Runge-Kutta yaklaşımı dalga klavuzlarındaki etkin kırılma indeksini üst tabakanın ve dalga klavuzunun yerel kırılma indeksine bağlı olarak hesaplamada kullanılır.

Bu çalışmada, kırılma indeksleri ve TE_{00} modlarındaki model alanlar hesaplandı. Hesaplanmış TE_{00} modları ışığın dalga klavuzu içindeki dağılımı

hakkında bilgi verir. Ayrıca, Runge-Kutta yaklaşımının kesinliđi test edildi.
Runge-Kutta yaklaşımının avantajları ve dezavantajları tartışıldı.

Anahtar Kelimeler: Elektirik Alanı, Dalga Klavuzu, Nümerik Simülasyon,
Runge-Kutta

ACKNOWLEDGEMENTS

I would like to acknowledge gratefully to my supervisor Assoc. Prof. Dr. Serhat Çakır for his guidance, discussions, support, and encouragement during this thesis.

I would also like to thank to my family for their supports and encouragements.

TABLE OF CONTENTS

ABSTRACT	iii
ÖZ.....	v
ACKNOWLEDGEMENTS.....	vii
TABLE OF CONTENTS.....	viii
LIST OF FIGURES.....	x
CHAPTER	
1. INTRODUCTION.....	1
1.1. REVIEW OF WAVE PHYSICS.....	3
1.2. INTERFERENCE OF WAVES.....	5
2. GRADED INDEX WAVEGUIDES.....	9
2.1. INTRODUCTION.....	9
2.2. THE EIKONAL EQUATION.....	10
2.3. MODAL ANALYSIS OF A PARABOLIC INDEX FIBER.....	14
2.4 PULSE DISPERSION.....	18
3. BASIC THEORY.....	28
4. NUMERICAL METHODS.....	35
4.1. THE EULER METHOD.....	35
4.2. THE RUNGE-KUTTA METHOD.....	36

5. NUMERICAL SOLUTION OF WAVE EQUATION.....	40
6. CONCLUSIONS.....	49
REFERENCES.....	51

LIST OF FIGURES

FIGURES

1.1	Integrated optical Mach-Zehnder interferometer. (a) evanescent waves into super- and substrate with coordinates and refractive index profile $n(x)$. (b) in- and outcoupled light	2
1.2	Configuration of a conventional Mach-Zehnder interferometer	6
2.1	Graded index profile.....	9
2.2	A graded-index material can be modeled as a stack of thin layers, each with index $n(x)$	11
2.3	Variation of $\tau(\tilde{\beta})$ with $\tilde{\beta}$ for $q = 0.25$	20
2.4	Variation of $\tau(\tilde{\beta})$ with $\tilde{\beta}$ for $q = 1.98$	21
2.5	Variation of $\tau(\tilde{\beta})$ with $\tilde{\beta}$ for $q = 2$	21
2.6	Variation of $\tau(\tilde{\beta})$ with $\tilde{\beta}$ for $q = \infty$	22

2.7 Variation of $\Delta\tau_1$ and $\Delta\tau_2$	26
5.1 E^2 versus x at $y = 0.5$	43
5.2 E^2 versus x at $y = 1$	43
5.3 E^2 versus x at $y = 1.5$	44
5.4 E^2 versus x at $y = 2$	44
5.5 E^2 versus x at $y = 2.5$	45
5.6 E^2 versus x at $y = 3$	45
5.7 E^2 versus x at $y = 3.5$	46
5.8 E^2 versus x at $y = 4$	46
5.9 E^2 versus x at $y = 4.5$	47
5.10 E^2 versus x at $y = 5$	47

CHAPTER 1

INTRODUCTION

Electromagnetic waves may be regarded, from communications point of view, as divisible into two main types, free waves and guided waves. The radiation from a dipole situated in free space is an example of the first type; waves on a parallel wire line are of the second type. The energy of free waves spreads out more or less in all directions in space, but in a guided wave it is confined to the vicinity of the guiding system. Thus, by suitable choice of the guiding system, energy may be transferred from place to place with little loss.

A waveguide can be defined as any structure capable of guiding the flow of electromagnetic energy in a direction parallel to its axis, while substantially confining it to a region either within or adjacent to its surfaces.

The theoretical treatment of the propagation of light in waveguides using Maxwell's equations yields differential equations which can be analytically solved for a constant refractive index of the medium, which is

propagated by the light, and its environment. In the case of surface waveguides, only the superstrate exhibits a constant refractive index. The waveguide itself represents a gradient profile of the refractive index. Thus, only the differential equation, which describes the evanescent field in the area of the superstrate, can be solved analytically. In the area of the waveguide itself, approximation methods must be used, since the refractive index varies along an axis incident into the waveguide.

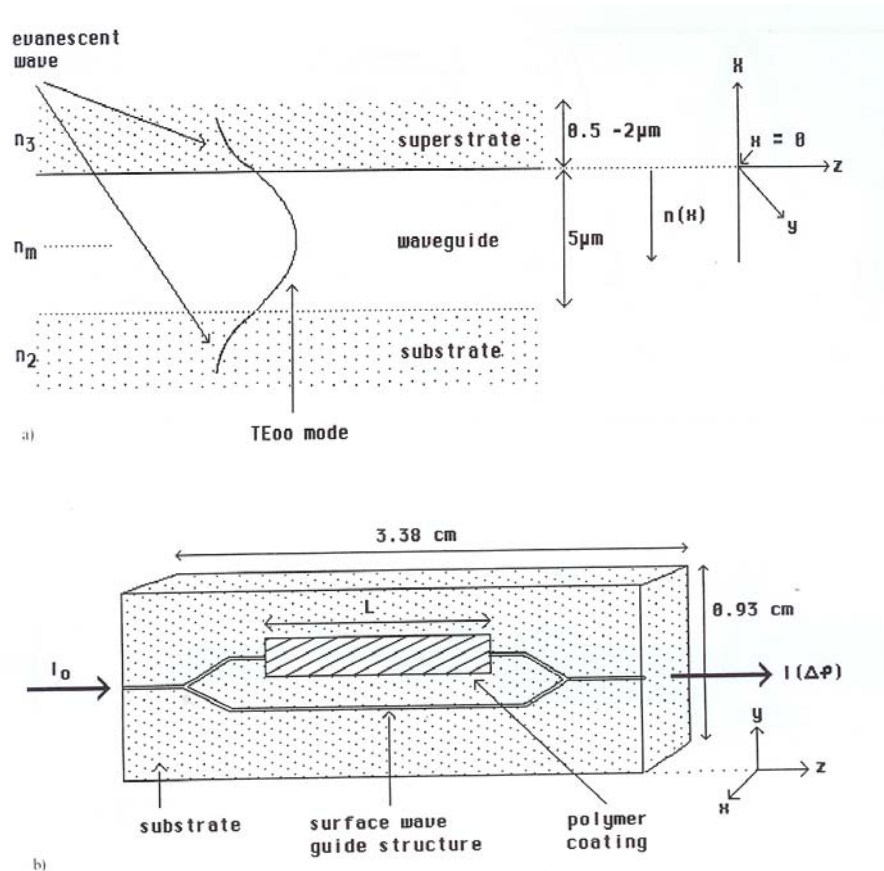


Figure 1.1 Integrated optical Mach-Zehnder interferometer. (a) evanescent waves into super- and substrate with coordinates and refractive index profile $n(x)$, (b) in- and outcoupled light

The model fields are connected by so-called effective indices. This effect can be monitored by use of interferometric principles. In the case of waveguides the so-called March-Zehnder interferometers are used. The incident radiation I_0 is split into two arms. One is covered by a superstrate which is a thin polymer film. This superstrate influences the propagation in one of the arms. Thus, after reunion of the two partial electromagnetic waves, the resulting intensity shifted in phase (Fig.1.1).

1.1 REVIEW OF WAVE PHYSICS

Periodic disturbance propagating through the medium or vacuum is called wave. If the displacement of every point on string oscillates sinusoidally, it is called monochromatic wave.

Light wave is an electromagnetic wave. Electric $\left(\vec{E}\right)$ and magnetic $\left(\vec{B}\right)$ fields oscillate simultaneously. Light waves can propagate in a vacuum or in media. Electric field is plotted to represent wave oscillations.

Maxwell's equations for electric and magnetic fields in vacuum;

$$\nabla \cdot \vec{E} = 0 \qquad \nabla \cdot \vec{B} = 0 \qquad (1.1)$$

$$\nabla \times \vec{E} = -\frac{\partial \vec{B}}{\partial t} \qquad \nabla \times \vec{B} = \mu_0 \epsilon_0 \frac{\partial \vec{E}}{\partial t} \qquad (1.2)$$

Wave equation are obtained from curl ($\nabla \times$) of equations (1.2) using identity

$$\nabla \times \nabla \times E = \nabla(\nabla \cdot E) - \nabla^2 E.$$

$$\nabla^2 E = \mu_0 \varepsilon_0 \frac{\partial^2 E}{\partial t^2} \quad (1.3)$$

$$\nabla^2 B = \mu_0 \varepsilon_0 \frac{\partial^2 B}{\partial t^2} \quad (1.4)$$

Here μ_0 is permeability of vacuum and ε_0 is permittivity of vacuum.

Wave phase velocity is $v_{phase} = \lambda * f$. Fundamental wave propagation equation is defined as

$$\frac{\partial^2 y(x,t)}{\partial x^2} = \frac{1}{v_{ph}^2} \frac{\partial^2 (x,t)}{\partial t^2}. \quad (1.5)$$

The general solutions to wave equation is $y(x,t) = F(x \pm v_{phase} t)$ where $F()$ is any arbitrary function.

General solution to wave equation is

$$E(x,t) = E_0 \sin(kx - \omega t), \text{ where } k = 2\pi / \lambda, \omega = 2\pi f. \quad (1.6)$$

Wave accelerates any nearby charge in the y direction; power is deposited into charge y -degree of freedom. This wave is said to be *polarized* along y .

Wave carries energy. Power carried by wave across unit area is;

$$P(x,t) = c\epsilon_0 |E(x,t)|^2 = c\epsilon_0 E_0^2 \text{Sin}^2(kx - \omega t) \quad (1.7)$$

If the wave is y -polarized then power deposited along y direction. If the wave is x -polarized then power has E_x and E_y components.

$$(P \propto E_x^2 + E_y^2)$$

Time-averaged power over one wave cycle is

$$\langle P(x,t) \rangle = c\epsilon_0 E_0^2 \langle \text{Sin}^2(kx - \omega t) \rangle = \frac{c\epsilon_0 E_0^2}{2}. \quad (1.8)$$

For a single monochromatic wave, time-averaged power is independent of time and position.

$$\langle P \rangle = P_0 = c\epsilon_0 E_0^2 / 2 \quad (1.9)$$

1.2 INTERFERENCE OF WAVES

Interferometer is a device, which splits light waves into two components, which travel different paths and recombine after some relative

propagation phase delay $\nabla\phi$. There are a lot of kinds of interferometer. One of them is Mach-Zehnder interferometer.

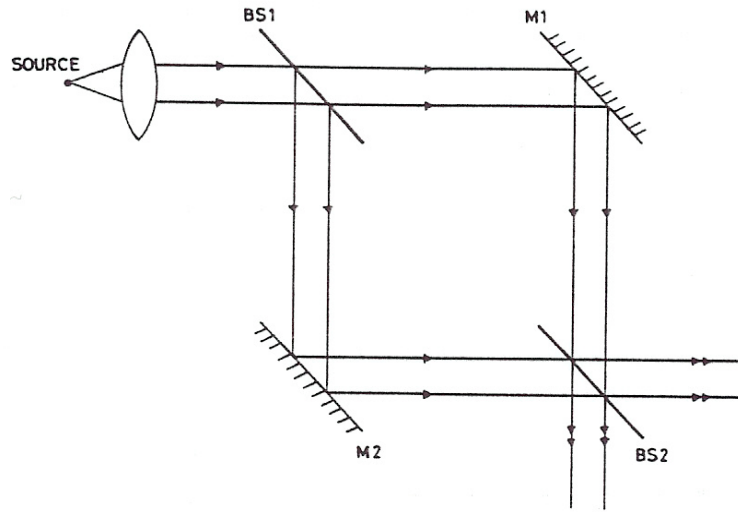


Figure 1.2 Configuration of a conventional Mach-Zehnder interferometer.

Figure 1.2 shows a conventional Mach-Zehnder interferometer using bulk optical elements in which light from a source is first split into two arms with a beam splitter and then recombined by another beam splitter after propagating through two different arms. Depending on the phase difference between the two arms, at the output of the interferometer one obtains an interference pattern much like in any other interferometer.

If input wave is

$$\vec{E}_m = E_0 \hat{y} \sin(kx - wt), \quad (1.10)$$

then splitted waves are

$$\vec{E}_1(x, t) = E_1 \hat{y} \sin(kx - wt) \quad (1.11)$$

and

$$\vec{E}_2(x, t) = E_2 \hat{y} \sin(kx - wt + \Delta\phi), \quad (1.12)$$

where $E_1^2 + E_2^2 = E_0^2$.

When these waves recombine, wave equation becomes;

$$\vec{E}_{out}(x, t) \hat{y} [E_1 \sin(kx - wt) + E_2 \sin(kx - wt + \Delta\phi)] \quad (1.13)$$

According to $\langle P(x, t) \rangle = c\epsilon_0 \langle |E(x, t)|^2 \rangle$, time-averaged power of output wave

can be computed as;

$$\begin{aligned} \langle P(x, t) \rangle &= c\epsilon_0 \left[\frac{E_1^2}{2} + \frac{E_2^2}{2} + \langle 2E_1E_2 \sin(kx - wt + \phi) \rangle \right] \\ &= c\epsilon_0 \left[\frac{E_1^2}{2} + \frac{E_2^2}{2} + E_1E_2 \langle \cos(\phi) - \cos(2kx - 2wt + \phi) \rangle \right] \\ &= P_1 + P_2 + 2\sqrt{P_1P_2} \cos\phi \end{aligned} \quad (1.14)$$

If $P_1 = P_2 = P$ (%50-%50 power split) then

$$\langle P \rangle = 2P(1 + \cos \Delta\phi) = \frac{I_0}{2}(1 + \cos \Delta\phi) \quad (1.15)$$

where I_0 is detector power when $\Delta\phi = 0$.

Plot of detector power vs. phase shift is called “Interferogram”.

When monochromatic waves of identical wavelength interfere, the interferogram is periodic with period $\Delta\phi = 2\pi$ over the entire domain $\Delta\phi = [-\infty, \infty]$. These waves are said to interfere “coherently”[1].

Consider light source containing many wavelengths λ_i . If this light passes through Mach-Zehnder interferometer of path imbalance ΔL , relative phase shift between waves of length λ_i is $\Delta\phi(\lambda_i) = 2\pi\Delta L / \lambda_i$.

Bright and dark fringes from various wavelengths overlap, ‘smearing’ the interferogram; a smeared interferogram is the interference of light with “finite coherence”.

CHAPTER 2

GRADED INDEX WAVEGUIDES

2.1 INTRODUCTION

Waveguides with a continuously varying index are referred to as a graded index waveguides (Figure 2.1) [2].

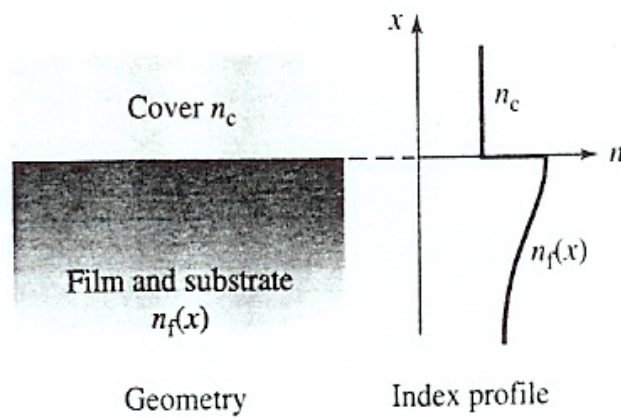


Figure 2.1 Graded index profile

Graded index multimode fibers find important applications in local area networks and short-haul communication systems. In this chapter we discuss graded index fibers characterized by the following refractive index distribution

$$n^2(r) = n_1^2 \left[1 - 2b \left(\frac{r}{a} \right)^q \right]; \quad 0 < r < a$$

$$= n_2^2 = n_1^2(1 - 2b); \quad r > a \quad (2.1)$$

where r corresponds to a cylindrical radial coordinate, n_1 represents the value of the refractive index on the axis, n_2 represents the refractive index of the cladding, and b is the grading parameter; $q = 1$, $q = 2$, and $q = \infty$ correspond to the linear, parabolic, and step index profiles, respectively. Equation (2.1) describes what is usually referred to as a power law profile, which gives an accurate description of the refractive index variation in most multimode fibers. One of the main advantages of the power law profile is that by choosing different values of q one can describe a variety of profiles and in addition we can get rigorously correct expressions for the time taken by different rays to propagate through a certain distance of the fiber.

2.2 THE EIKONAL EQUATION

Ray propagation in a graded structure is described by the Eikonal equation. A simple construction based on Snell's law will be used. What

happens if a ray is launched in a graded-index material? The index gradient can be modeled as a series of microscopically thin homogeneous layers, each with an index $n(x)$, where x is a distance from the axis ($x = 0$) to the thin layer. Consider the ray incident upon the interface between layers $n(x)$ and $n(x + \Delta x)$ at an angle θ , as shown in Figure 2.2. This angle is the complement of the angle we normally use in applying Snell's law.

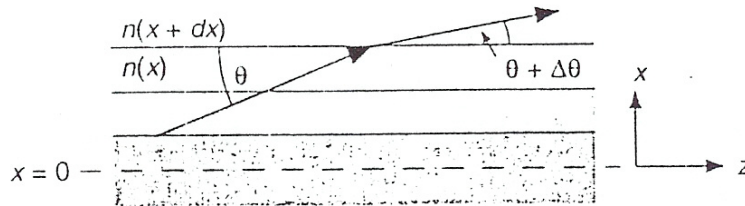


Figure 2.2 A graded-index material can be modeled as a stack of thin layers, each with index $n(x)$.

The ray refracts at the interface between two layers. In terms of θ as

we have defined it, Snell's law is:

$$n(x) \cos \theta = n(x + \Delta x) \cos(\theta + \Delta\theta) \quad (2.2)$$

The change in direction, $\Delta\theta$, is very small. The term $n(x + \Delta x)$ can be rewritten in terms of a Taylor series expansion of $n(x)$ around x :

$$n(x + \Delta x) \cong n(x) + \frac{dn}{dx} \Delta x \quad (2.3)$$

The $\cos(\theta + \Delta\theta)$ term can be expanded using the trigonometric identity

$$\cos(\theta + \Delta\theta) = \cos\theta \cos\Delta\theta - \sin\theta \sin\Delta\theta \approx \cos\theta - \sin\theta \Delta\theta \quad (2.4)$$

where we have assumed that $\cos\Delta\theta \approx 1$ and $\sin\Delta\theta \approx \Delta\theta$.

Plugging Equations 2.3 and 2.4 into Equation 2.2, we get

$$n(x) \cos\theta = \left[n(x) + \frac{dn}{dx} \Delta x \right] [\cos\theta - \sin\theta \Delta\theta] \quad (2.5)$$

Cancelling common terms and rearranging yields

$$n(x) \sin\theta \Delta\theta = \frac{dn}{dx} \cos\theta \Delta x - \frac{dn}{dx} \Delta x \sin\theta \Delta\theta \quad (2.6)$$

The last term in Equation 2.6, being a product of two infinitesimals, is negligible compared to the other terms, so Equation 2.6 can be written as

$$\frac{dn}{dx} \cong n(x) \tan\theta \frac{\Delta\theta}{\Delta x} \quad (2.7)$$

For most waveguide situations, the angle θ is going to be small, so

small angle approximations can be used to simplify the expression:

$$\tan \theta \cong \theta \cong \frac{\Delta x}{\Delta z} \quad (2.8)$$

Substitute this into Equation 2.7, noting that $\Delta x = \Delta z \tan \theta$:

$$\frac{dn}{dx} \cong n(x) \frac{\Delta \theta}{\Delta z}$$

$$\lim_{\Delta z \rightarrow 0} \frac{dn}{dx} = n(x) \frac{d}{dz}(\theta) = n(x) \frac{d}{dz} \left(\frac{dx}{dz} \right) \quad (2.9)$$

$$= n(x) \frac{d^2 x}{dz^2}$$

Finally, solve for $d^2 x / dz^2$:

$$\frac{d^2 x}{dz^2} = \frac{1}{n(x)} \frac{dn(x)}{dx} \quad (2.10)$$

This equation is called the Eikonal equation. The function $x(z)$ describes the exact ray path, and can be determined from Equation 2.10 once $n(x)$ is known. As a practical matter, when the index of refraction is not a strong function of position, the denominator term for $n(x)$ in Equation 2.10 is often replaced with n_0 , the index of refraction at $x = 0$.

$$\frac{d^2x}{dz^2} \approx \frac{1}{n(0)} \frac{dn(x)}{dx} \quad (2.11)$$

This assumption can make an otherwise intractable differential equation manageable, while introducing negligible error so long as $n(x)$ does not change considerably over the spatial extent of mode. The Eikonal equation states that the ray always bends toward the higher-index material.

2.3 MODAL ANALYSIS OF A PARABOLIC INDEX FIBER

The propagation characteristics of an infinitely extended parabolic index fiber characterized by the following refractive index variation

$$n^2 = n_1^2 \left[1 - 2b \left(\frac{r}{a} \right)^2 \right] \quad (2.12)$$

or, in Cartesian coordinates,

$$n^2 = n_1^2 \left[1 - 2b \frac{x^2 + y^2}{a^2} \right] \quad (2.13)$$

where b and a are constants and n_1 represents the axial refractive index.

If we substitute equation in the scalar wave equation we obtain

$$\nabla^2 \Psi = \frac{n_1^2}{c^2} \left[1 - 2b \left(\frac{x^2}{a^2} + \frac{y^2}{a^2} \right) \right] \frac{\partial^2 \Psi}{\partial t^2} \quad (2.14)$$

We assume a model solution of the form

$$\Psi(x, y, z, t) = \Psi(x, y)e^{i(\omega t - \beta z)} \quad (2.15)$$

The equation becomes

$$\frac{\partial^2 \Psi}{\partial x^2} + \frac{\partial^2 \Psi}{\partial y^2} + \left\{ k_0^2 n_1^2 \left[1 - 2b \left(\frac{x^2}{a^2} + \frac{y^2}{a^2} \right) \right] - \beta^2 \right\} \Psi = 0 \quad (2.16)$$

We used the method of separation of variables and write

$$\Psi(x, y) = X(x)Y(y) \quad (2.17)$$

If we substitute above solution in equation and divide by XY we obtain

$$\left(\frac{1}{X} \frac{d^2 X}{dx^2} - k_0^2 n_1^2 \frac{2b}{a^2} x^2 \right) + \left(\frac{1}{Y} \frac{d^2 Y}{dy^2} - k_0^2 n_1^2 \frac{2b}{a^2} y^2 \right) + (k_0^2 n_1^2 - \beta^2) = 0 \quad (2.18)$$

The variables have indeed separated out and we may write

$$\left(\frac{1}{X} \frac{d^2 X}{dx^2} - k_0^2 n_1^2 \frac{2b}{a^2} x^2 \right) = -K_1 \quad (2.19)$$

and

$$\left(\frac{1}{Y} \frac{d^2 Y}{dy^2} - k_0^2 n_1^2 \frac{2b}{a^2} y^2 \right) = -K_2 \quad (2.20)$$

where K_1 and K_2 are constants and

$$\beta^2 = k_0^2 n_1^2 - K_1 - K_2 \quad (2.21)$$

We now use the variables

$$\xi = \gamma x, \quad (2.22)$$

$$\eta = \gamma y \quad (2.23)$$

with

$$\gamma = \left[n_1 k_0 \frac{\sqrt{2b}}{a} \right]^{1/2} = \frac{\sqrt{V}}{a} \quad (2.24)$$

where

$$V = k_0 n_1 a (2b)^{1/2} \quad (2.25)$$

represents the waveguide parameter. Thus

$$\begin{aligned} d^2 X / d\xi^2 + (\Lambda_1 - \xi^2) X(\xi) &= 0 \\ d^2 Y / d\eta^2 + (\Lambda_2 - \eta^2) Y(\eta) &= 0 \end{aligned} \quad (2.26)$$

where

$$\Lambda_1 = \frac{K_1}{\gamma^2} \quad (2.27)$$

and

$$\Lambda_2 = \frac{K_2}{\gamma^2} \quad (2.28)$$

For bounded solutions -that is, for $X(\xi)$ and $Y(\eta)$ to and to zero as ξ , $\eta \rightarrow \pm\infty$ (i.e., $x, y \rightarrow \pm\infty$)- we must have

$$\Lambda_1 = 2m + 1; \quad m = 0, 1, 2, \dots \quad (2.29)$$

and

$$\Lambda_2 = 2n + 1; \quad n = 0, 1, 2, \dots \quad (2.30)$$

The corresponding model distributions $X(x)$ and $Y(y)$ are the Hermite-Gauss functions. Thus, we obtain the following expressions for mode profiles and corresponding propagation constants.

$$\Psi_{mn}(x, y) = \left[N_m H_m(\xi) e^{-\frac{1}{2}\xi^2} \right] \left[N_n H_n(\eta) e^{-\frac{1}{2}\eta^2} \right] \quad (2.31)$$

$$\beta_{mn} = k_0 n_1 \left[1 - \frac{2(m+n+1)}{k_0 n_1} \sqrt{\frac{2b}{a^2}} \right]^{\frac{1}{2}} \quad (2.33)$$

where $m, n = 0, 1, 2, \dots$ and

$$N_m = \left[\frac{\gamma}{2^m m! \sqrt{\pi}} \right]^{1/2} = \left[\frac{\sqrt{V}/a}{2^m m! \sqrt{\pi}} \right]^{1/2} \quad (2.34)$$

represent the normalization constant. Different values of m and n corresponding to different modes of the fiber. Equation 2.33 is an analytic solution of the propagation constant of the (m, n) th mode in such a fiber.

2.4 PULSE DISPERSION

One of the important characteristics of an optical waveguide is pulse dispersion, which is the temporal spreading of a pulse of light launched into the waveguide. One of the mechanisms that leads to pulse dispersion is the difference in time taken by different rays. Thus, if all rays are launched simultaneously in a waveguide, at the output the rays will arrive at different times and, hence, will correspond to a temporal dispersion of the pulse.

Dispersion along with attenuation determines the information-carrying capacity of the fiber optic system. As such, a study of the dispersion characteristics of an optical fiber is a subject of considerable importance.

Ray optics are used to study the dispersion characteristics. A ray is characterized by two invariants $\tilde{\beta}$ and \tilde{l} . The invariant $\tilde{\beta}$ is defined by the following equation

$$\tilde{\beta} = n(r)\cos\theta(r) \quad (2.35)$$

where $\theta(r)$ is the angle that the ray makes with the z-axis. The invariant $\tilde{\beta}$ is a consequence of the fact that the refractive index does not depend on the z-coordinate (translational invariance). The cylindrical symmetry (ϕ independence) leads to the invariant \tilde{l} , which is usually referred to as the skewness parameter. Meridional rays are characterized by $\tilde{l} = 0$; thus, all rays in a planer waveguide have zero skewness parameter [3].

The time taken by a ray to traverse a certain distance z through the optical fiber is

$$\tau(z) = \left[A\tilde{\beta} + \frac{B}{\tilde{\beta}} \right] z \quad (2.36)$$

where

$$A = \frac{2}{C(2+q)}, \quad B = \frac{qn_1^2}{c(2+q)} \quad (2.37)$$

c being the velocity of light in free space.

In Figures 2.3-2.6 $\tau(\tilde{\beta})$ have been plotted as a function of $\tilde{\beta}$ for

$$n_2 = 1.46, \quad \Delta = 0.01(\Rightarrow n_1 \approx 1.4748) \quad (2.38)$$

corresponding to

$$q = 0.25, 1.98, 2.00, \text{ and } \infty$$

respectively, with $n_2 < \tilde{\beta} < n_1$. The vertical axis gives the time taken by the ray to traverse a kilometer length of the fiber.

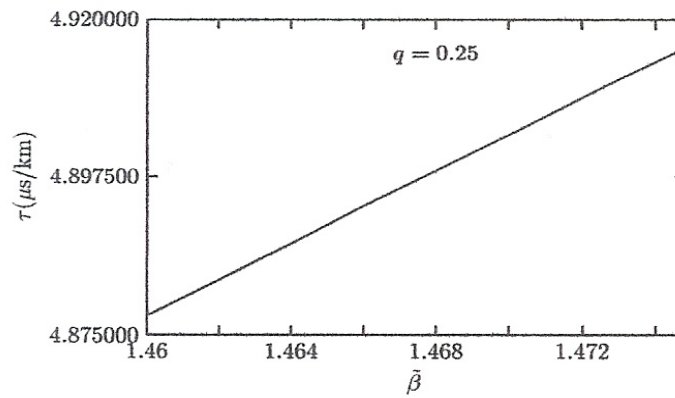


Figure 2.3 Variation of $\tau(\tilde{\beta})$ with $\tilde{\beta}$ for $q = 0.25$

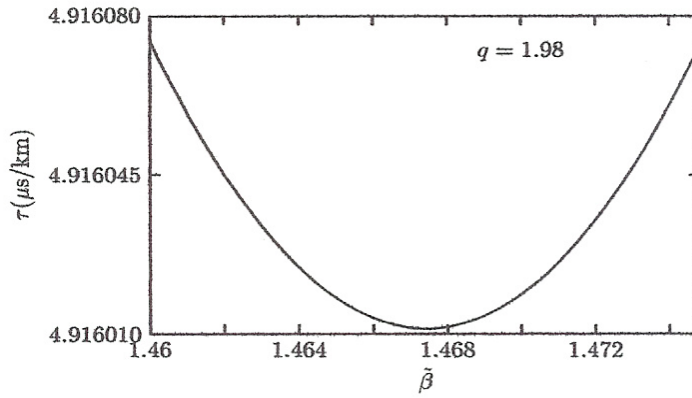


Figure 2.4 Variation of $\tau(\tilde{\beta})$ with $\tilde{\beta}$ for $q = 1.98$

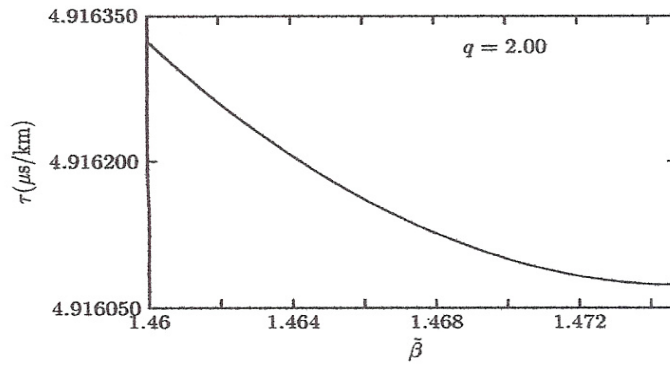


Figure 2.5 Variation of $\tau(\tilde{\beta})$ with $\tilde{\beta}$ for $q = 2.00$

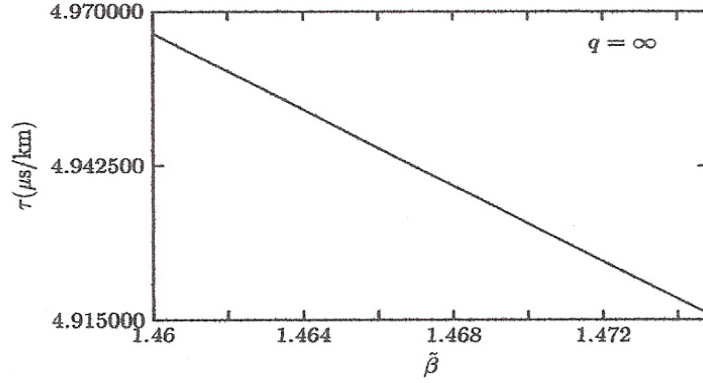


Figure 2.6 Variation of $\tau(\tilde{\beta})$ with $\tilde{\beta}$ for $q = \infty$.

We consider some specific cases:

Case1: $q = \infty$ (step index fibers). For $q = \infty, A = 0, B = \frac{n_1^2}{c}$. Thus,

$$\tau(\tilde{\beta}) = \frac{n_1^2}{c\tilde{\beta}} z \quad (2.39)$$

represent a monotonically decreasing function of $\tilde{\beta}$ (see Figure 2.6). Since

$n_2 < \tilde{\beta} < n_1$, we get

$$\tau_{\max} = \tau(\tilde{\beta} = n_2) = \frac{n_1^2}{cn_2} z$$

which corresponds to the ray that is incident at the core-cladding interface at the critical angle. Further

$$\tau_{\min} = \tau(\tilde{\beta} = n_1) = \frac{z}{c/n_1}$$

which corresponds to the ray propagating parallel to the z-axis. Thus, the pulse dispersion is given by

$$\begin{aligned} \Delta\tau = \tau_{\max} - \tau_{\min} &= \frac{n_1}{c} \frac{(n_1 - n_2)}{n_2} L \\ &\approx \frac{n_1 \Delta}{c} L \end{aligned} \quad (2.40)$$

For $n_1 \approx 1.46, \Delta \approx 0.01$ we obtain

$$\Delta\tau \approx 50 \text{ ns/km}$$

Case2: $q=2$ (parabolic index fibers). For

$q = 2, A = 1/2c, B = n_1^2/2c$. Thus

$$\tau(\tilde{\beta}) = \frac{1}{2c} \left[\tilde{\beta} + \frac{n_1^2}{\tilde{\beta}} \right] z \quad (2.41)$$

which is again a monotonically decreasing function of $\tilde{\beta}$ for $n_2 < \tilde{\beta} < n_1$ (see Figure 2.5). Indeed

$$\tau_{\max} = \tau(\tilde{\beta} = n_2) = \frac{1}{2c} \left[n_2 + \frac{n_1^2}{n_2} \right] z$$

and

$$\tau_{\min} = \tau(\tilde{\beta} = n_1) = \frac{z}{c/n_1}$$

giving the following expression for pulse dispersion

$$\Delta\tau = \tau_{\max} - \tau_{\min} \approx \frac{n_2\Delta^2}{2c} z \quad (2.42)$$

For $n_1 \approx 1.46$, $\Delta \approx 0.01$ we obtain

$$\Delta\tau \approx \frac{1}{4} \text{ ns/km}$$

Case3: The optimum profile. From analysis of a parabolic index fiber, we find that there is a tremendous decrease in the pulse dispersion as we go from a step index fiber to a parabolic index fiber. To obtain the optimum value of q corresponding to a minimum pulse dispersion, we first note that for $n_2 < \tilde{\beta} < n_1$, $\tau(\tilde{\beta})$ is a monotonically increasing or decreasing function except for the values of q given by

$$2 - 4\Delta < q < 2$$

This can be easily shown by finding the value of $\tilde{\beta}$ for which $d\tau/d\tilde{\beta} = 0$. The condition immediately gives

$$A - \frac{B}{\tilde{\beta}_m^2} = 0 \Rightarrow \tilde{\beta}_m = \sqrt{\frac{B}{A}} = n_1 \sqrt{\frac{q}{2}} \quad (2.43)$$

Since for guided rays $n_2 < \tilde{\beta} < n_1$ and $n_2 = n_1 \sqrt{1 - 2\Delta}$, the value of $\tilde{\beta}$ given by Equation 2.43 lies in the range $n_2 < \tilde{\beta} < n_1$ only for $2 - 4\Delta < q < 2$. For $q > 2$, $\tau(\tilde{\beta})$ decreases monotonically as $\tilde{\beta}$ increases from n_2 to n_1 and the pulse dispersion is given by

$$\begin{aligned} \Delta\tau(q > 2) &= \tau(\tilde{\beta} = n_2) - \tau(\tilde{\beta} = n_1) \\ &= \frac{(n_1 - n_2)}{c(q + 2)} \left(\frac{qn_1}{n_2} - 2 \right) z \end{aligned} \quad (2.44)$$

For $q < 2 - 4\Delta$, $\tau(\tilde{\beta})$ increases monotonically as $\tilde{\beta}$ increases from n_2 to n_1 and the corresponding pulse dispersion is given by

$$\begin{aligned} \Delta\tau(q < 2 - 4\Delta) &= \tau(\tilde{\beta} = n_1) - \tau(\tilde{\beta} = n_2) \\ &= \frac{(n_1 - n_2)}{c(q + 2)} \left(2 - \frac{qn_1}{n_2} \right) z \end{aligned} \quad (2.45)$$

Finally

$$\Delta\tau(2 - 4\Delta < q < 2) = \text{Max}(\Delta\tau_1, \Delta\tau_2) \quad (2.46)$$

where

$$\Delta\tau_1 = \tau(\tilde{\beta} = n_2) - \tau(\tilde{\beta} = \tilde{\beta}_m) \quad (2.45)$$

$$\Delta\tau_2 = \tau(\tilde{\beta} = n_1) - \tau(\tilde{\beta} = \tilde{\beta}_m) \quad (2.46)$$

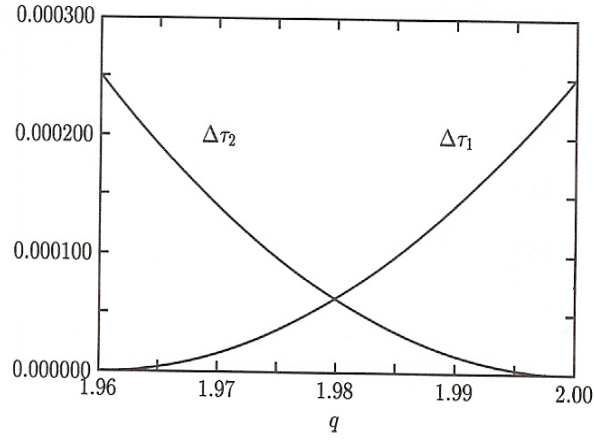


Figure 2.7 Variation of $\Delta\tau_1$ and $\Delta\tau_2$

Figure 2.7 shows the plots of $\Delta\tau_1$ and $\Delta\tau_2$ as a function of q in the domain $2 - 4\Delta < q < 2$. Obviously, the point of intersection the two curves corresponds to minimum pulse dispersion. This point of intersection corresponds to $\Delta\tau_1 = \Delta\tau_2$ - that is, $\tau(\tilde{\beta} = n_2) = \tau(\tilde{\beta} = n_1)$ - which implies

$$q = \frac{2n_2}{n_1} = 2\sqrt{1 - 2\Delta} \approx 2 - 2\Delta \quad \text{optimum profile} \quad (2.47)$$

The corresponding pulse dispersion is given by

$$\Delta\tau \approx \frac{n_1}{8c} \Delta^2 z \quad (2.48)$$

Thus, for $n_1 \approx 1.46$ and $\Delta = 0.01$ we get

$$\begin{aligned} \Delta\tau &\approx 50 \text{ ns/km} && \text{for } q = \infty \\ &\approx \frac{1}{4} \text{ ns/km} && \text{for } q = 2 \\ &\approx \frac{1}{16} \text{ ns/km} && \text{for } q = 1.98 \end{aligned} \quad (2.49)$$

CHAPTER 3

BASIC THEORY

The propagation of light in the arms of the waveguides can be expressed in terms of the Maxwell equations:

$$\vec{\nabla} \times \vec{E} = -\frac{1}{c} \frac{\partial \vec{B}}{\partial t} = -\frac{1}{c} \mu \frac{\partial \vec{H}}{\partial t} \quad (3.1)$$

$$\vec{\nabla} \times \vec{H} = \frac{1}{c} n^2 \left(\vec{r} \right) \frac{\partial \vec{E}}{\partial t} \quad (3.2)$$

$$\vec{\nabla} \cdot \left(n^2 \left(\vec{r} \right) \vec{E} \right) = 0 \quad (3.3)$$

$$\vec{\nabla} \cdot \vec{B} = 0 \quad (3.4)$$

where we have used the constitutive relation

$$\vec{B} = \mu \vec{H} \quad (3.5)$$

in which $\vec{E}, \vec{B}, \vec{H}$ represent the electric field, magnetic induction, and magnetic intensity, respectively.

Now taking the curl of Equation (3.1) and using Equation (3.2) we get

$$\vec{\nabla} \times (\vec{\nabla} \times \vec{E}) = -\frac{1}{c} \mu \frac{\partial}{\partial t} (\vec{\nabla} \times \vec{H}) = -\frac{1}{c^2} \mu n^2(\vec{r}) \frac{\partial^2 \vec{E}}{\partial t^2}$$

or

$$\vec{\nabla} (\vec{\nabla} \cdot \vec{E}) - \nabla^2 \vec{E} = -\frac{1}{c^2} \mu n^2(\vec{r}) \frac{\partial^2 \vec{E}}{\partial t^2} \quad (3.6)$$

Further

$$\vec{\nabla} \cdot (n^2(\vec{r}) \vec{E}) = \vec{\nabla} n^2(\vec{r}) \cdot \vec{E} + n^2(\vec{r}) \vec{\nabla} \cdot \vec{E} = 0$$

Thus

$$\vec{\nabla} \cdot \vec{E} = -\frac{1}{n^2(\vec{r})} \vec{\nabla} n^2(\vec{r}) \cdot \vec{E} \quad (3.7)$$

Substituting in Equation (3.6) we obtain

$$\vec{\nabla} \left(-\frac{1}{n^2(\vec{r})} \vec{\nabla} n^2(\vec{r}) \cdot \vec{E} \right) - \nabla^2 \vec{E} = -\frac{\mu}{c^2} n^2(\vec{r}) \frac{\partial^2 \vec{E}}{\partial t^2}$$

$$\nabla^2 \vec{E} - \frac{\mu n^2(\vec{r})}{c^2} \frac{\partial^2 \vec{E}}{\partial t^2} = \vec{\nabla} \left(-\frac{1}{n^2(\vec{r})} \nabla n^2(\vec{r}) \cdot \vec{E} \right) \quad (3.8)$$

In a similar manner, taking the curl of the Equation (3.2) and using Equation (3.1) we get

$$\begin{aligned} \vec{\nabla} \times (\vec{\nabla} \times \vec{H}) &= \frac{1}{c} \vec{\nabla} \times \left(n^2(\vec{r}) \frac{\partial \vec{E}}{\partial t} \right) = \frac{1}{c} \left(n^2(\vec{r}) \vec{\nabla} \times \frac{\partial \vec{E}}{\partial t} + \vec{\nabla} n^2(\vec{r}) \times \frac{\partial \vec{E}}{\partial t} \right) \\ &= \frac{1}{c} n^2(\vec{r}) \frac{\partial}{\partial t} \left(-\frac{\mu}{c} \frac{\partial \vec{H}}{\partial t} \right) + \frac{1}{c} \vec{\nabla} n^2(\vec{r}) \times \left(\frac{c}{n^2(\vec{r})} \vec{\nabla} \times \vec{H} \right) \end{aligned}$$

or

$$\vec{\nabla} (\vec{\nabla} \cdot \vec{H}) - \nabla^2 \vec{H} = -\frac{1}{c^2} n^2(\vec{r}) \mu \frac{\partial^2 \vec{H}}{\partial t^2} - \frac{1}{n^2(\vec{r})} \vec{\nabla} \times \vec{H} \times (\vec{\nabla} n^2(\vec{r})) \quad (3.9)$$

Further

$$\vec{\nabla} \cdot \vec{B} = \vec{\nabla} \cdot (\mu \vec{H}) = 0$$

Thus

$$\mu \vec{\nabla} \cdot \vec{H} = 0 \quad (3.10)$$

Substituting in Equation (3.9) we obtain

$$\nabla^2 \vec{H} = \frac{1}{c^2} n^2(\vec{r}) \mu \frac{\partial^2}{\partial t^2} \vec{H} + \frac{1}{n^2(\vec{r})} \vec{\nabla} \times \vec{H} \times \left(\vec{\nabla} n^2(\vec{r}) \right) \quad (3.11)$$

So,

$$\left[\nabla^2 - \frac{\mu n^2(\vec{r})}{c^2} \frac{\partial^2}{\partial t^2} \right] \begin{Bmatrix} \vec{E} \\ \vec{H} \end{Bmatrix} = \begin{Bmatrix} \text{grad} \left[\frac{\vec{E}}{n^2(\vec{r})} \left[\text{grad} \left(n^2(\vec{r}) \right) \right] \right] \\ \frac{1}{n^2(\vec{r})} \left[\text{rot} \vec{H} \right] \times \left[\text{grad} \left(n^2(\vec{r}) \right) \right] \end{Bmatrix} \quad (3.12)$$

where ∇^2 is the Laplace operator

The above equations show the inhomogeneous wave equations.

If the variation of $n^2(\vec{r})$ within the distance of one optical wavelength is small, the solution of the homogeneous wave Equations (3.13) are good approximation for the solutions of inhomogeneous Equations (3.12) also. With $\mu = 1$ one obtains

$$\left[\nabla^2 - \frac{n^2(\vec{r})}{c^2} \frac{\partial^2}{\partial t^2} \right] \begin{Bmatrix} \vec{E} \\ \vec{H} \end{Bmatrix} = 0 \quad (3.13)$$

A translational invariance exists with respect to the z axis, taking into account that along this axis the parameters of the material do not change and the extension of the waveguide in the z axis is much more than in the x and y axes and the parameters of the material depend on the frequency; thus:

$$\vec{E}(\vec{r}, t) = \vec{E}(x, y) e^{i(k_z z - \omega t)}$$

$$\vec{B}(\vec{r}, t) = \vec{B}(x, y) e^{i(k_z z - \omega t)} \quad (3.14)$$

From Equation 3.13

$$\frac{\partial^2 E}{\partial x^2} + \frac{\partial^2 E}{\partial y^2} + \frac{\partial^2 E}{\partial z^2} - \frac{n^2(\vec{r})}{c^2} \frac{\partial^2 E}{\partial t^2} = 0$$

$$\frac{\partial^2 E}{\partial z^2} = -k_z^2 E(x, y) e^{i(k_z z - \omega t)} = -k_z^2 \vec{E}$$

$$\frac{\partial^2 E}{\partial t^2} = \omega^2 E(x, y) e^{i(k_z z - \omega t)} = \omega^2 \vec{E}$$

so,

$$\frac{\partial^2 E}{\partial x^2} + \frac{\partial^2 E}{\partial y^2} - k_z^2 \vec{E} + \frac{n^2(\vec{r})}{c^2} \omega^2 \vec{E} = 0 \quad (3.15)$$

using the correlations

$$k_0 = \frac{\omega}{c},$$

$$k_z = k_0 n_{eff},$$

$$\nabla_t^2 = \frac{\partial^2}{\partial x^2} + \frac{\partial^2}{\partial y^2}$$

we get,

$$\left[\nabla_t^2 + k_0^2 \left(n^2(\vec{r}) - n_{eff}^2 \right) \right] \vec{E} = 0 \quad (3.16)$$

In a similar manner,

$$\left[\nabla_t^2 + k_0^2 \left(n^2(\vec{r}) - n_{eff}^2 \right) \right] \vec{B} = 0 \quad (3.17)$$

In the case of a stripe waveguide the general solutions can be obtained by the partial differential equations of the transversal electric and the transversal magnetic wave. Thus Equations (3.16) and (3.17) can be reduced to a scalar wave equations. Just the E_y component must be calculated by

reducing to problem with respect to a propagation in the z direction. The following equation is generally valid for a stripe waveguide:

$$\frac{\partial^2 E_y(x, y)}{\partial x^2} + \frac{\partial^2 E_y(x, y)}{\partial y^2} + k_0^2 \left(n^2(\vec{r}) - n_{eff}^2 \right) E_y(x, y) = 0 \quad (3.18)$$

The waveguide considered was produced by ion implantation, thus the refractive index in Equation (3.18) depends on x and y :

$$\frac{\partial^2 E_y(x, y)}{\partial x^2} + \frac{\partial^2 E_y(x, y)}{\partial y^2} + k_0^2 \left(n(x, y)^2 - n_{eff}^2 \right) E_y(x, y) = 0 \quad (3.19)$$

This equation cannot be solved anatically. It represents an eigenvalue equation for the model field E_y with the eigenvalues n_{eff} .

$$E_y(x, y) = E_y(x) \cdot E_y(y) \quad (3.20)$$

Therefore Equation (3.19) can be separated into

$$\frac{\partial^2 E_y(x)}{\partial x^2} + k_0^2 \left[n(x, y)^2 - n_{eff}^2(y) \right] E_y(x) = 0 \quad (3.21.a)$$

$$\frac{\partial^2 E_y(y)}{\partial y^2} + k_0^2 \left[n_{eff}^2(y) - n_{eff}^2 \right] E_y(y) = 0 \quad (3.21.b)$$

$n_{eff}(y)$ gives the so-called horizontal effective index profile.

CHAPTER 4

NUMERICAL METHODS

4.1 THE EULER METHOD

In order to understand the Euler Method, first consider a single differential equation of the type

$$\frac{\partial y}{\partial t} = f(y, t). \quad (4.1)$$

For the derivative on the left-hand side

$$\frac{y(t+h) - y(t)}{h} + O(h) = f(y, t), \quad (4.2)$$

or

$$y(t+h) = y(t) + hf(y(t), t) + O(h^2). \quad (4.3)$$

If we ignore the error term $O(h^2)$, then (4.3) becomes a recursion formula which allows us to compute the function $y(t)$, starting from an initial value $y(0)$, in steps of h .

The Euler Method is certainly easy to understand, but it is not very accurate and not very stable. At each application of the recursion one moves along the tangents to the solution curves up to the next mesh point. One therefore overshoots the target slightly at each pass [4].

4.2 THE RUNGE-KUTTA METHOD

The well-known Runge-Kutta algorithm permits the numeric solution of differential equation. It belongs to the single step methods; which means that for the calculation of a y_{k+1} value only the information from the interval $[y_k, y_{k+1}]$ is used. The accuracy of the procedure strongly depends on the distance h of the interval. Such a method is particularly useful if certain coefficients in the differential equation are empirical functions for which analytical expressions are not known, and hence for which initial series developments are not feasible. In place of using values of N derivatives of y at one point, it uses values only of the first derivative at N suitable chosen points.

The derivation of the basic formulas may be illustrated by considering the special case when second-order accuracy in h is required. We consider a first order differential equation of the type

$$\frac{dy}{dt} = f(y,t) \quad (4.4)$$

In order to be able to apply the technique of the Taylor expansion, we shall assume in what follows that $f(y,t)$ is differentiable a sufficient number of times with respect to y and t . Then, writing down the first few terms of the Taylor expansion of $y(t)$ and applying (4.4), we obtain

$$\begin{aligned} y(t+h) &= y(t) + h \frac{dy(t)}{dt} + \frac{h^2}{2} \frac{d^2 y(t)}{dt^2} + O(h^3) \\ &= y(t) + hf(y(t),t) + \frac{h^2}{2} \frac{df(y(t),t)}{dt} + O(h^3) \end{aligned} \quad (4.5)$$

To differentiate $f(y,t)$ with respect to t we apply

$$f'(x) = \frac{f(x+h) - f(x)}{h} + O(h) \quad (4.6)$$

so,

$$\frac{df(y(t),t)}{dt} = \frac{f(y(t+h),t+h) - f(y(t),t)}{h} + O(h), \quad (4.7)$$

and replace the quantity $y(t+h)$ in (4.7) using (4.3). Substitution in (4.5)

leads to

$$y(t+h) = y(t) + h \frac{f(y(t), t) + hf(y(t), t), t+h) + f(y(t), t)}{2} + O(h^3) \quad (4.8)$$

For practical computation one often introduces the following abbreviations:

$$\begin{aligned} k_1 &= f(y(t), t), \\ k_2 &= f(y(t) + hk_1, t+h) \end{aligned} \quad (4.9)$$

In this abbreviated notation the formula for the improved the Euler method is as follows:

$$y(t+h) \cong y(t) + \frac{h}{2}(k_1 + k_2) + O(h^3) \quad (4.10)$$

The best known of the methods obtained in this way is the Runge-Kutta method.

By methods analogous to that just given, similar formulas giving higher order accuracy in h may be obtained.

Third-order accuracy:

$$y(t+h) \cong y(t) + \frac{h}{6}(a_1 + 4a_2 + a_3)$$

$$a_1 = f(y(t), t)$$

$$a_2 = f\left(y(t) + \frac{1}{2}a_1, t + \frac{1}{2}h\right)$$

$$a_3 = f(y(t) + 2a_2 - a_1, t + h)$$

Fourth-order accuracy:

$$y(t+h) = y(t) + \frac{h}{6}(b_1 + 2b_2 + 2b_3 + b_4)$$

$$b_1 = f(y(t), t)$$

$$b_2 = f\left(y(t) + \frac{1}{2}b_1, t + \frac{1}{2}h\right)$$

$$b_3 = f\left(y(t) + \frac{1}{2}b_2, t + \frac{1}{2}h\right)$$

$$b_4 = f(y(t) + b_3, t + h)$$

CHAPTER 5

NUMERICAL SOLUTION OF WAVE EQUATION

Recall the equations (3.21.a) and (3.21.b)

$$\frac{\partial^2 E_y(x)}{\partial x^2} + k_0^2 [n(x, y)^2 - n_{eff}^2(y)] E_y(x) = 0 \quad (3.21.a)$$

$$\frac{\partial^2 E_y(y)}{\partial y^2} + k_0^2 [n_{eff}^2(y) - n_{eff}^2] E_y(y) = 0 \quad (3.21.b)$$

As it is said before, the waveguide itself represents a gradient profile of the refractive index. So, in the area of the waveguide, approximation methods must be used, since the refractive index varies along an axis incident into the waveguide.

The solution of the differential equation within the waveguide can be found in the following way: First, the waveguide is split into 10-20 vertical

and 10-20 horizontal stripes. For every point, we can find $n(x,y)$ using equation (5.1)

$$n(x, y) = 0.5e^{-a[(x-2.5)^2 + (y-2.5)^2]} + 1 \quad (5.1)$$

where

$$\begin{aligned} n(x, y) &= n_0 e^{-a(x^2 + y^2)} \\ \frac{n(x, y)}{n_0} &= 0.1 = e^{-a(5^2 + 5^2)} \\ a &= 0.0461 \end{aligned}$$

For a certain y_i the value $n(x, y_i)$ only depends on x . Therefore, the calculated values $n_{eff}(y_i)$ belong to a corresponding model field at the stripe element y_i . We can find $n_{eff}(y_i)$ using equation (5.2)

$$n_{eff}(y) = \frac{\int_0^5 \left(0.5e^{-0.0461[(x-2.5)^2 + (y-2.5)^2]} + 1 \right) dx}{5} \quad (5.2)$$

In a similar manner,

$$n_{eff} = \frac{\int_0^5 \int_0^5 \left(0.5e^{-0.0461[(x-2.5)^2 + (y-2.5)^2]} + 1 \right) dx dy}{25} \quad (5.3)$$

Runge-Kutta algorithm permits the numerical solutions of these differential equations. When applied to waveguides for the solution of Eqn.3.21a it must

be assumed that the refractive index stays constant within the area of the superstrate, then

$$n(x, y) = n_{\text{sup}} = \text{cont.} \quad (5.4)$$

Within the superstrate, the differential equation can be solved in a closed form. Therefore, at the position $x = 0$ (interface / waveguide to superstrate) a connection condition exists and the solution of the differential equation within the waveguide must be solved such that the electric field can be continuously differentiated. This connection condition can be derived from the Maxwell equations and is given by

$$\frac{dE_y(x, y_i)}{dx} = E_y(0, y_i) k_0^2 \sqrt{n_{\text{eff}}^2(y_i) - n_{\text{sup}}^2} \quad \text{at } x = 0 \quad (5.5)$$

where n_{sup} represents the refractive index outside the waveguide in the superstrate.

Then, we use the following starting conditions of the Runge-Kutta algorithm. The field becomes zero and the slope of the field is taken to be 0.000001 at the origin.

From there, we find the electric fields in the waveguide. Graphs show the square of electric fields at different positions.

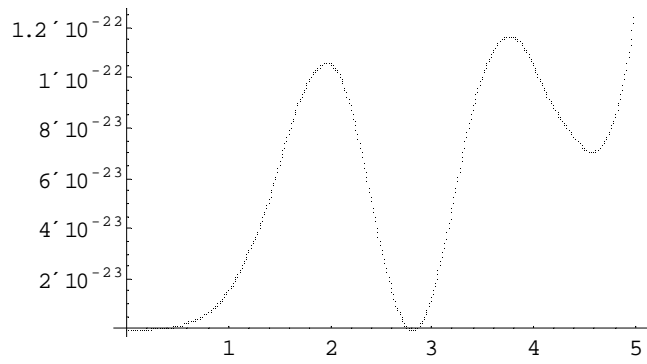


Figure 5.1 E^2 versus x at $y = 0.5 \mu m$

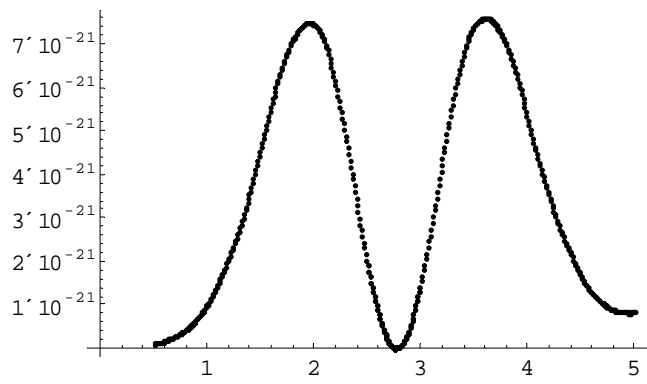


Figure 5.2 E^2 versus x at $y = 1 \mu m$

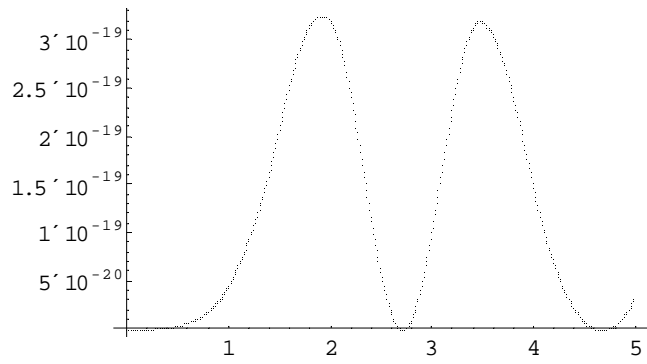


Figure 5.3 E^2 versus x at $y = 1.5 \mu m$

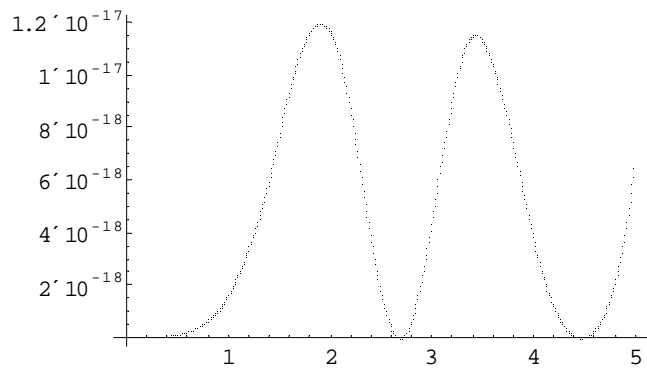


Figure 5.4 E^2 versus x at $y = 2 \mu m$

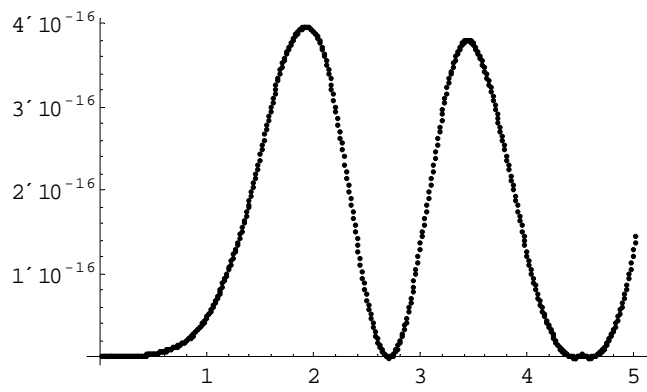


Figure 5.5 E^2 versus x at $y = 2.5 \mu m$

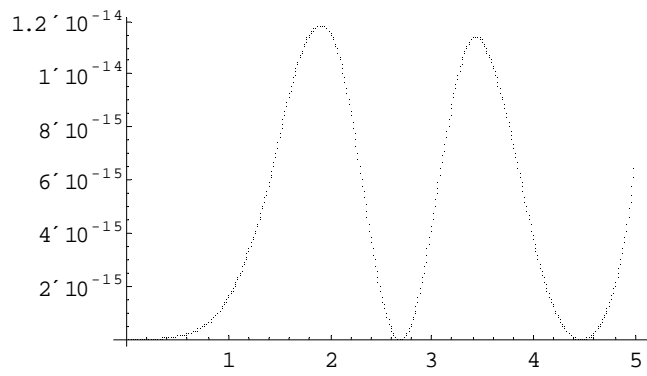


Figure 5.6 E^2 versus x at $y = 3 \mu m$

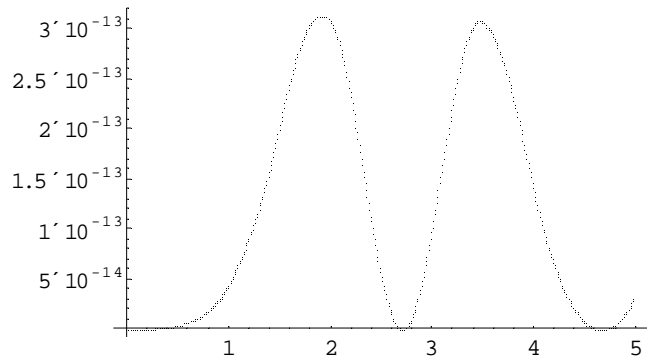


Figure 5.7 E^2 versus x at $y = 3.5 \mu m$

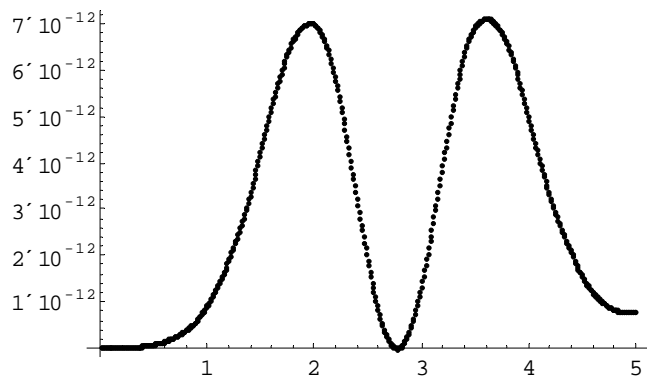


Figure 5.8 E^2 versus x at $y = 4 \mu m$

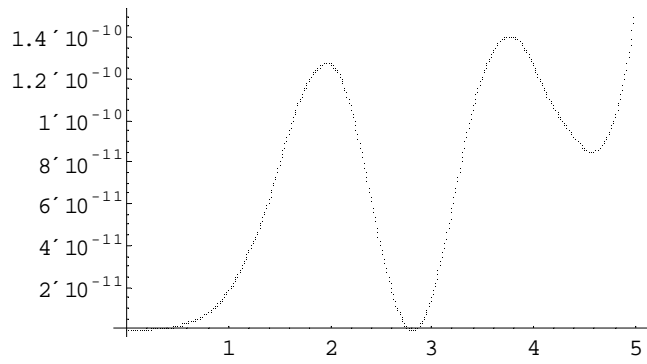


Figure 5.9 E^2 versus x at $y = 4.5 \mu m$

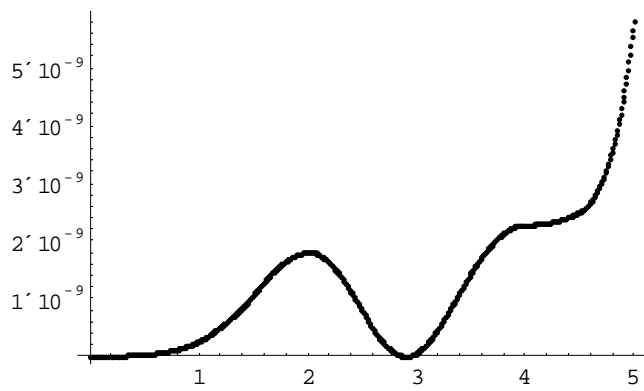


Figure 5.10 E^2 versus x at $y = 5 \mu m$

The above figures show the E^2 versus x at different y positions. There are two peaks at about $x = 2 \mu m$ and $x = 3.5 \mu m$. The peak values of E^2 are

different at different y positions. We expect that the value of E^2 is maximum in the middle of the waveguide and it is minimum at the edge of the waveguide. The numerical errors propagate at $y = 1 \mu m$, $y = 1.5 \mu m$, $y = 3.5 \mu m$, $y = 4 \mu m$ are small. But they are big at $y = 0.5 \mu m$, $y = 2 \mu m$, $y = 2.5 \mu m$, $y = 3 \mu m$, $y = 4.5 \mu m$, $y = 5 \mu m$.

CHAPTER 6

CONCLUSIONS

As mentioned above, the covering of one arm in a Mach-Zehnder configuration causes a phase shift of the propagating wave in this measuring arm with respect to the other. For this reason, the superstrate will influence the phase modulated intensity at the output of the Mach-Zehnder interferometer in dependence on the resulting Δn_{eff} .

The theoretical treatment of the propagation of light in waveguides using Maxwell's equations yields differential equations which can be analytically solved for a constant refractive index of the medium, which is propagated by the light, and its environment. In the case of surface waveguides, only the superstrate exhibits a constant refractive index. The waveguide itself represents a gradient profile of the refractive index. Thus, only the differential equation, which describes the evanescent field in the area of the superstrate, can be solved analytically. In the area of the waveguide

itself, approximation methods must be used, since the refractive index varies along an axis incident into the waveguide.

In this study, we used the Runge-Kutta approximations. Runge-Kutta approximations permit the precalculation of optimal parameters such as the refractive index of the polymer, the refractive index of stripe waveguide and the model fields. However, to obtain good simulations by the Runge-Kutta the approximation must be applied at least one hundred times. For this reason, the Runge-Kutta method is very time consuming.

REFERENCES

- (1) Hecht, E. And Zajac, A., *Optics*, Addison Wesley, 1988.
- (2) Chin-Lin Chen, *Elements of Optoelectronics and Fiber Optics*, 1996
- (3) A. Ghatak, K. Thyagarajan, *Introduction to Fiber Optics*, 1998.
- (4) Erich W. Schmid, Gerhard Spitz, Wolfgang Lösch, *Theoretical Physics on the Personal Computer*, Second Edition, 1987.
- (5) John A. Buck, *Fundamentals of Optical Fibers*, 1995.
- (6) B. Drapp, G. Gauglitz, J. Ingenhoff, “*Simulation of Transversal Modal Fields in Integrated Optic Components*”, *Analytica Chimica Acta*, 265 (1992) 267-275.
- (7) R. Syms, J. Cozens, *Optical Guided Waves and Devices*, 1992
- (8) John M. Senior, *Optical Fiber Communications Principles and*

Practice, Second Edition, 1992.

- (9) Martha L. Abell, James P. Braselton, *Differential Equation with
Mathematica*, 1993.